Proceeding of the IEEE
International Conference on Robotics and Biomimetics
Dali, China, December 2019

Principle and Control Method of Energy Input in Dynamic Walking of Humanoid Robots*

Xiang Luo, Yufeng He and Xingjing Zhao
School of Mechanical Engineering
Southeast University
Jiangning district, Nanjing 211189, China
luox@seu.edu.cn

***Abstract* - Pushing ground with trailing leg to gain energy is the main way of energy input for biped robots. This paper studies the control method of ground-push in dynamic walking of biped robots. First, the principle of the ground-push is studied. Second, the implement method of ground-push, which is for a 27 DOF humanoid robot, and under a decentralized control architecture, is developed. At final, the proposed method is verified in the simulation. The results show that the proposed method achieves stable walking, and the performance of speed control is satisfied.**

Index Terms – Humanoid, Dynamic walking, ground-push, gait planning.

I. INTRODUCTION

The Passive Dynamics based Walking (PDW) implies the more efficient utilization of energy in biped walking. The PDW can be traced to their earlier prototypes called passive walkers, such as the work of McGeer [1]. From then on, a number of studies, such as that of Ruina [2], were conducted on principles of biped walking by designing and testing passive walking machines. In 2005, Collins et al. [3] presented new types of walking machines, namely, passive dynamics based walking machines, in which simple actuation and control are used to substitute for the role of gravity in passive walking. Their research revealed that the efficiency of the dynamic walkers to be at a level almost as high as human walking. However, these machines can only perform straight walking with constant speeds due to their few degrees of freedom (DOFs). In addition, with simplified models and mathematical methods, some scholars have made important achievements in revealing the basic mechanism of dynamic walking, such as the work of Goswami [4].

The successive goal is to develop theories and methods so as to implement the PDBW on humanoid robots which have much more DOFs than the mentioned passive dynamic walkers. Grizzle et al. [5,6] and Westervelt et al. [6] introduced the concept and method of virtual constraints, which are holonomic constraints on the robot's configuration by feedback control. The control coordinates the evolution of the various links of the robot throughout a particular phase, which reduces the DOFs of dominant dynamics. The concept of hybrid zero dynamics [6] denoted the convergence nature of a dimension-reduced space of the biped robots by ways of feedback control, which provided an idea to implement the virtual constraints. Based on these, Grizzle and Chevallereau [7] proposed an approach for 3D biped robots. In their work, three strategies were developed to ensure stable walking: first, a stability condition was imposed in the search for an optimal gait; second, an event-based controller was designed to modify the eigenvalues of the Poincaré map; and third, a pertinent choice of outputs on hybrid zero dynamics was proposed, which ensured the walking stability.

Our group have been working on exploring principles and control methods of dynamic walking. First, we proposed a two-point-foot gait for 2D dynamic walking [8], in which the behavior of foot is modeled as two ground-contact points at heel and toe respectively. Second, a 3D control method for sensor-based dynamic walking was studied [9]. Recently, the influence of torso motion on performance of walking is approached, and a torso control method is integrated into walking control of a 27 DOF humanoid robot [10].

In a walking cycle, the double support phase (DSP) is the main phase of energy input. Ground-push of rear leg is the external form of energy input of the robot, while the coordinated motion and work of the related joints are the internal mechanism of energy input. This paper will study the principle and control method of energy input in walking, and verify the validity through simulation.

II. MODEL OF 27-DOF HUMANOID ROBOT

The robot in this study comprises 27 DOFs, including six DOFs in the Working Coordination System (WCS), six DOFs in each leg, three DOFs in each arm, and 3 DOFs in the waist, as shown in Fig. 1. The robot has similar mass distribution ratios to humans, of which, the upper body accounts for approximately 70% of the total mass, and each leg for approximately 15%, as shown in Table 1.

To describe the pose of the robot conveniently, a fixed coordinate system of the robot (RCS) at the centre of mass of the robot torso is defined, as shown in Fig. 1. Another important coordinate system, called Planning Coordinate System (PCS), is also established. The origin of PCS coincides with that of the RCS, the Y-axis points to the desired walking direction, the Z-axis goes upward, and the X-axis is determined by the right-handed rule. The gait is planned in the PCS. The planning result is transformed into the RCS, and then is solved to obtain the motion in the joint space.

* This work is supported by the National Natural Science Foundation of China under grants 51075071 and 51375085.

978-1-7281-6321-5/19//$31.00 ©2019 IEEE

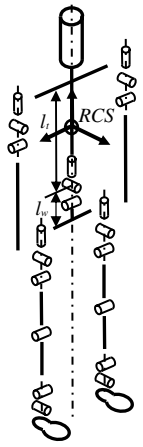

Fig. 1. Biped robot.

Table 1. Parameters of robot

Total height l_{total}	1.40m	Width of foot l_{wf}	0.08m
Length of torso l_t	0.40m	Total mass m_t	30kg
Width of shoulder l_s	0.30m	Mass of torso m_{tor}	15kg
Width of hip l_h	0.15m	Mass of pelvis m_{pel}	5kg
Height of waist l_w	0.10m	Mass of thigh m_{th}	1.25kg
Length of arm l_a	0.60m	Mass of calf m_c	1.25kg
Length of thigh l_{th}	0.35m	Mass of foot m_f	1kg
Length of calf l_c	0.35m	Mass of arm m_a	1.5kg
Length of foot l_f	0.135m		

III. PRINCIPLE OF DYNAMIC WALKING

A. Principle of dynamic walking

Dynamic walking control is the combination of passive motion and active control. On the one hand, passive motion is the key to improve the walking efficiency of the robot. The main passive process is the passive tilting motion of the robot with the landing foot as the fulcrum in the single support phase. On the other hand, active control is comprised of several aspects to maintain the walking stability of the robot, including virtual constraints to maintain the trunk posture in passive motion, swing leg trajectory and landing position control to maintain the periodic walking cycle of the robot, and pedal control to adjust the walking speed.

We regard that the function structure of a foot can be simplified as two ground-contact points at heel and toe respectively. The two-point-foot walking pattern [8] follows two principles: Only one contact point of the stance foot contacts with the ground at any moment in the single support phase (SSP). Therefore, the SSP is comprised of two segments of passive falling movements: heel support and toe support.

B. Hybrid dynamics of biped walking

The walking cycle of a robot is divided into several phases, and the switching between the phases is triggered by the sensor signal, as shown in Fig. 2. Because of the different forms of constraints, the dynamics are different at each phase. Different simplified models can be used to describe the phases of walking, so biped walking is a process of hybrid dynamics.

In the sagittal plane, a walking cycle includes SSP, landing impact phase (LIP) and DSP. Here, the LIP refers to the period from the start of landing of the swing leg to the moment when the ground reaction force crosses the peak value. First, in the SSP, the torso and pelvis posture of the robot is maintained upright through the control of the waist and the hip joint of the supporting leg. The length of the front leg keeps constant, due to the knee is controlled fixed. Further, the influence of swing leg is regarded as disturbance. Therefore, the robot is modelled with an inverted pendulum with centralized mass. Second, in the impact phase, the reaction force of the ground is larger, and the torso posture of the robot will suddenly change because of the impact. Therefore, the model of the two-level inverted pendulum is adopted, in which the superior represents the torso considering its mass and rotational inertia, and the inferior represents the legs without mass. Third, in the phase of double support, the robot will accelerate tilting due to the ground-push of the rear leg. A two-level inverted pendulum model with external driving force is adopted.

In the frontal plane, the one-level inverted pendulum model is used to describe the dynamics because the motion amplitude of the robot in the frontal plane is much smaller than that in the sagittal plane.

IV. CONTROL METHOD FOR DYNAMIC WALKING

A. Coordination mechanism of dynamic walking

Passivity is a characteristic of dynamic walking robots. Therefore, it is appropriate to select an index related to passive motion to organize the motion control of the robot. In this paper, the tilting angle of the robot (TAR), which is the angle of the line from the heel of the support foot to the mass centre of the torso in the sagittal plane, is used as the reference variable of walking control. Further, the walking control is sensor based. A walking period consists of several ordered phases, and the switching between them is triggered by sensor signals, as shown in Fig. 2.

In this study, the mass and rotational inertia of the torso

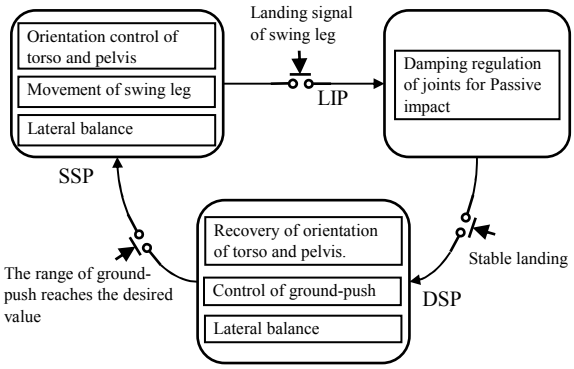

Fig. 2. Control diagram of dynamic biped walking.

of the robot are absolutely dominant in the whole robot, so the disturbance force generated by the movement of other limbs is much smaller than that of the torso itself. The motion planning of the robot is decomposed into three aspects: combination motions of torso-pelvis-supporting legs, motion of swing leg and motion of arms. The coordinated motion among these motions is achieved because these motions all use the TAR as independent variable.

Gait planning has the following aspects, as shown in Fig. 3. Whether in single or double support, the control goal of the combination of torso-pelvis-support leg (or front leg in DSP) is to maintain the posture of the torso and pelvis of the robot. The walking control is mainly the adjustment of speed and step length.

B. Energy input and distribution

By the ground-push of the rear leg, the reaction force of the ground drives the robot to swing around the foot of the leading leg, and hence inputs momentum. During this process, the torques of the robot joints are internal forces, which can distribute the momentum over the robot, for example, deliver the momentum to the torso which has the majority of mass to hold it. Certainly, the redistribution of momentum can be achieved at any phases of walking. In a single support, the process of swinging legs is also a redistribution of momentum, by which part of the momentum of the torso is transformed to that of leg swing.

C. Regulation of speed

The walking control is mainly the adjustment of speed and step length. First, the speed control is achieved by adjusting the ground-push force, which is a PD law, according to the error between the desired speed and the actual speed, as shown in Fig. 3. Meanwhile, the step length is automatically regulated according to the average speeds, with a predetermined relationship [9].

D. lateral balance

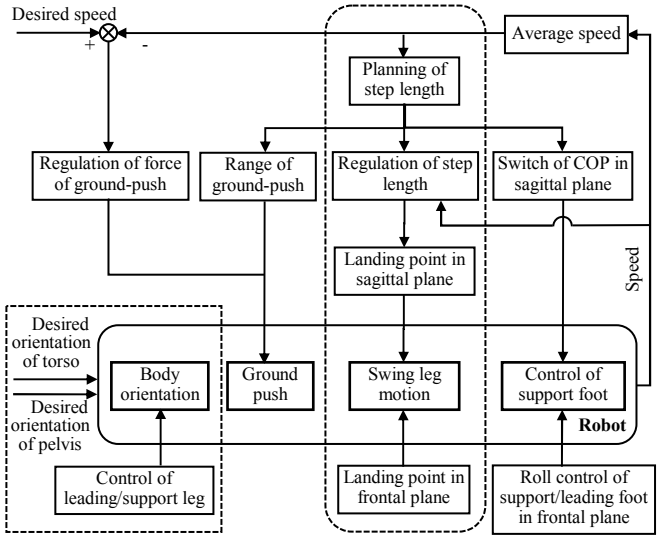

Fig. 3. Diagram of distribution control of humanoid robot

The principle of lateral balance is of two folds: first, plan lateral landing point according to the orientation sensor before landing; second, regulate the centre of pressure (COP) of the support foot after landing. The details can be found in [9].

V. PRINCIPLE AND CONTROL OF GROUND-PUSH

A. Dynamics of Dimensional Reduction Model

In the DSP of stable biped walking, the motion of the robot is a passive dominated movement, which is mainly dominated by inertia and gravity, because the torso has the absolute dominant momentum. The goal of active control is to create a controllable passive dominated movement. First, the torso and pelvis posture are controlled by the waist and hip joints to maintain the stability of the robot. Second, the motion is restrained to inverted pendulum motion by the control of the front leg. The control strategy is: the waist regulates the orientation of the torso, the hip maintains the orientation of pelvis, the knee holds on at full extension, and the ankle is under-actuated to ensure the heel in the contact with the ground. These constraints reduce the dimension of the robot to an inverted pendulum model in the sagittal plane, as illustrated in Fig. 4. Details about control of robot orientation and the front leg will be presented in VI.

It is hoped that the ground-push momentum can be fully translated into the momentum of the torso, which is perpendicular to the swing direction of the robot. To achieve this, the extension line of the reaction force from the ground must pass through the mass centre of the torso.

Assuming that the support foot maintains stable contact with the ground, the dynamics can be written as,

$$ml\dot{v}+mgl\sin\left(\frac{\varphi}{2}\right)=fl\sin(\varphi)\,, \tag{1}$$

where, m is the robot mass, l is the theoretic leg length, φ is the angle between legs, v is the speed of the torso mass in the sagittal plane, and f is the ground-push force.

B. Regulation law of ground-push force

In this paper, the regulation of input energy is carried out once a step. The magnitude of the force is regulated by a discrete PD algorithm as,

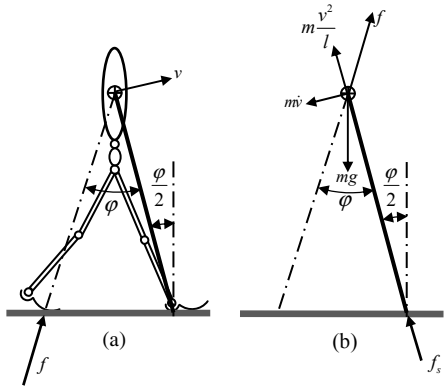

Fig. 4. Illustration of energy input. (a) Direction of reaction force points to mass center of torso. (b) Dynamics at ground-push moment.

$$f(i) = f(i-1) + k_p\left[v_d(i-1) - v_a(i-1)\right] + k_d\left[\dot{v}_d(i-1) - \dot{v}_a(i-1)\right], \quad (2)$$

where, i denotes the sequence of step, k_p and k_d are the control parameters, v_d and v_a the desired and the actual average speeds. Considering that

$$\dot{v}_d(i-1) \approx \frac{1}{T}\left[v_d(i-1) - v_d(i-2)\right],$$

where T denotes the step period, and

$$\dot{v}_a(i-1) \approx \frac{1}{T}\left[v_a(i-1) - v_a(i-2)\right],$$

we have,

$$f(i) = f(i-1) + \left[(k_1 + k_2) \quad -k_2\right]\begin{bmatrix} v_d(i-1) - v_a(i-1) \\ v_d(i-2) - v_a(i-2) \end{bmatrix}, \quad (3)$$

where, $k_1 = k_p$, and $k_2 = \frac{k_d}{T}$.

To ensure the leading leg in contact with the ground, the magnitude of the ground-push of the trailing leg must be confined. As shown in Fig. 4, the condition of force balance along the leading leg can be formulated as,

$$f_s + m\frac{v^2}{l} + f\cos(\varphi) - mg\cos(\frac{\varphi}{2}) = 0, \quad (4)$$

where, the contact force of the leading leg should fulfil that $f_s \geq 0$. Therefore, the ground-push force is constrained by a discrete formula as,

$$f(i) \leq \frac{1}{\cos\left(\varphi(i-1)\right)}\left[mg\cos\left(\frac{\varphi(i-1)}{2}\right) - m\frac{v^2(i-1)}{l}\right]. \quad (5)$$

C. Direction control of ground-push force

The desired direction of the ground-push force is directed from the COP of the foot of the trailing leg to the mass centre of the torso, as shown in Fig. 5(a). It can be described by a vector as,

$$\boldsymbol{f} = f\frac{\overline{PO}}{\left|\overline{PO}\right|}. \quad (6)$$

In order to transmit the ground reaction force to the trunk along the desired direction, the direction of the ground reaction force must be controlled. One way is to apply active torque at the relative joints, which include the ankle joint, the hip joints of the trailing leg, and the waist joints, to balance the reaction torque due to the ground-push. During the ground-push, the knee joint is controlled to be fixed. Further, the roll joint at ankle is not actuated, to ensure the stable contact of the sole with the ground.

The Jacobi matrix from the joints of the trailing leg and waist to the contact point of the foot can be calculated by,

$$J_p = \left[\boldsymbol{z}_a \times \overline{AP} \quad \boldsymbol{z}_{thy} \times \overline{HP} \quad \boldsymbol{z}_{thr} \times \overline{HP} \quad \boldsymbol{z}_{thp} \times \overline{HP} \quad \boldsymbol{z}_{wy} \times \overline{WP} \quad \boldsymbol{z}_{wr} \times \overline{WP} \quad \boldsymbol{z}_{wp} \times \overline{WP}\right], \quad (7)$$

where, $\boldsymbol{z}_a$ denotes the direction vector of the ankle joint in the PCS, $\boldsymbol{z}_{thy}, \boldsymbol{z}_{thr}, \boldsymbol{z}_{thp}$ are the direction vectors of the yaw, roll and pitch joints at the hip in the PCS respectively, and

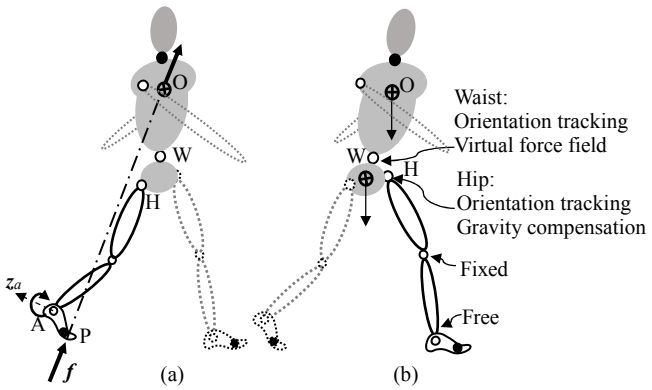

Fig. 5. Control in ground-push. (a) Control of trailing leg. (b) Orientation control of torso and pelvis.

$\boldsymbol{z}_{wy}, \boldsymbol{z}_{wr}, \boldsymbol{z}_{wp}$ are the direction vectors of the yaw, roll and pitch joints at the waist in the PCS respectively. Hence, we can obtain the control torques of the joints as,

$$\begin{bmatrix} \tau_a & \tau_{thy} & \tau_{thr} & \tau_{thp} & \tau_{wy} & \tau_{wr} & \tau_{wp} \end{bmatrix}^T = -J_p^T \boldsymbol{f}, \quad (8)$$

here,

$$\boldsymbol{\tau}_{push\_w} = \begin{bmatrix} \tau_{wy} & \tau_{wr} & \tau_{wp} \end{bmatrix}^T \quad (9)$$

is just part of the driving torque in the waist, and the other part will be calculated for orientation control of the torso in VI.

VI. Orientation Control of Robot Body

A. Self-orientated walking planning

In this research, the walking planning is carried out with respect to the PCS, as is similar to the navigation of ships which are orientated by compasses, is called self-orientated planning.

The body control includes the orientation control of the torso and pelvis, and the control of the supporting leg (or the leading leg in the DSP) which is the linkage part between the pelvis and the ground. In this study, the torso remained upright for the sake of simplicity. The pelvis, which provides a reference platform for the movement of the two legs, is expected upright during walking.

B. Orientation planning

The orientation transform matrix from the PCS to the WCS is ${}^{WCS}R = {}^{WCS}R_{RCS}\ {}^{RCS}R$, where ${}^{WCS}R_{RCS}$ denoting the orientation of the RCS with respect to the WCS.

A group of Euler angles, $\Theta = \begin{bmatrix} \alpha & \beta & \gamma \end{bmatrix}^T$ which denote a serial of relative rotations in the sequence of $\boldsymbol{z}_{pcs} \rightarrow (-\boldsymbol{y}_{pcs}) \rightarrow \boldsymbol{x}_{pcs}$ with respect to the PCS, is used to describe the orientation of the limbs. Hence, the orientation matrix of limb can be calculated by,

$${}^{pcs}R = \text{kinematics}(\Theta) = \begin{bmatrix} c\alpha c\beta & -c\alpha s\beta s\gamma - s\alpha c\gamma & -c\alpha s\beta c\gamma + s\alpha s\gamma \\ s\alpha c\beta & -s\alpha s\beta s\gamma + c\beta c\gamma & -s\alpha s\beta c\gamma - c\alpha s\gamma \\ s\beta & c\beta s\gamma & c\beta c\gamma \end{bmatrix}, \quad (10)$$

where $s\bullet$, $c\bullet$ denote $sin(\bullet)$ and $cos(\bullet)$ respectively. To the robot in fig. 1, the configuration of all the 3-DOF joints, including the waist, the hips shoulders, conform to the sequence. Taking the waist joint for example, the Euler angles are equal to the actual angles of the rotation axes with the definition that the initial angles of the axes, with which the torso is parallel to the pelvis, are zero.

Due to the influence during landing and ground-push, the orientation of the torso and pelvis are inevitably disturbed. In order to ensure the periodic stability of the walking cycle, in each SSP or DSP, the torso and pelvis are driven back to the desired orientation before the end of the phase.

C. Orientation control of torso in PCS

The orientation error of the torso is,

$$\Delta R_{tor} = (R_{tor})^{\mathrm{T}} R_{tor,d} = \begin{bmatrix} r_{11} & r_{12} & r_{13} \\ r_{21} & r_{22} & r_{23} \\ r_{31} & r_{32} & r_{33} \end{bmatrix}, \tag{11}$$

where, R_{tor} and $R_{tor,d}$ are the actual and desired orientations of the torso in the PCS respectively. The above error matrix can be transformed into an error vector as,

$$\boldsymbol{\varepsilon}_{tor} = \psi_{tor} \boldsymbol{a}_{tor} \ , \tag{12}$$

where, $\psi_{tor} = \arccos(0.5r_{11} + 0.5r_{22} + 0.5r_{33} - 0.5)$, and

$$\boldsymbol{a}_{tor} = \begin{bmatrix} a_x \\ a_y \\ a_z \end{bmatrix} = \frac{1}{2\sin(\psi_{tor})} \begin{bmatrix} r_{32} - r_{23} \\ r_{13} - r_{31} \\ r_{21} - r_{12} \end{bmatrix}$$

denote the angle and the direction axis of the rotation error respectively. Without consideration of the change of the direction axis, the derivative of the error can be written as,

$$\dot{\boldsymbol{\varepsilon}}_{tor} = \dot{\psi}_{tor} \boldsymbol{a}_{tor} \ . \tag{13}$$

In this paper, we use a combination of PD control plus control of virtual force field. First, the tracking torque in the PCS generated by PD rule is,

$$\boldsymbol{\tau}_{tr\_w\_pcs} = (k_{p\_w} \psi_{tor} + k_{d\_w} \dot{\psi}_{tor}) \boldsymbol{a}_{tor} \ , \tag{14}$$

where, k_{p_w} , k_{d_w} are proportional and derivative coefficients respectively. Second, the waist is used to imitate an inverted force field, whose magnitude is several times the gravity of the torso. The torque in the PCS is calculated by,

$$\boldsymbol{\tau}_{vf\_w\_pcs} = k_{vf} m_{tor} (\overline{OW} \times \boldsymbol{g}) \ , \tag{15}$$

where, $k_{vf} \geq 1$ is the multiple to the gravitational field, $\overline{OW}$ the vector pointing from the mass center of torso to the waist joint, and $\boldsymbol{g}$ the acceleration vector of gravity in the PCS, as shown in Fig. 5 (b). By (14) and (15), the driving torque in the PCS is,

$$\boldsymbol{\tau}_{s\_w\_pcs} = \boldsymbol{\tau}_{tr\_w\_pcs} + \boldsymbol{\tau}_{vf\_w\_pcs} \ . \tag{16}$$

Therefore, the corresponding torque in the joint space of the waist can be calculated by,

$$\boldsymbol{\tau}_{s\_w} = \begin{bmatrix} \boldsymbol{z}_{wy} & \boldsymbol{z}_{wr} & \boldsymbol{z}_{wp} \end{bmatrix}^{-1} \boldsymbol{\tau}_{s\_w\_pcs} \ . \tag{17}$$

Considering (9), the total driving torque in the joints of the waist is,

$$\boldsymbol{\tau}_{w} = \boldsymbol{\tau}_{push\_w} + \boldsymbol{\tau}_{s\_w} \ . \tag{18}$$

D. Orientation control of pelvis

Similar to the control of waist, the torque for orientation tracking of the pelvis at the hip of the leading leg is,

$$\boldsymbol{\tau}_{tr\_lh\_pcs} = (k_{p\_lh} \psi_{pel} + k_{d\_lh} \dot{\psi}_{pel}) \boldsymbol{a}_{pel} \ , \tag{19}$$

where, ψ_{pel} , $\boldsymbol{a}_{pel}$ are the angle and the direction vector of the error from the desired orientation to the actual one respectively, and k_{p_lh} , k_{d_lh} are the control parameters. The compensation torque for the gravity of torso and pelvis is,

$$\boldsymbol{\tau}_{gr\_lh\_pcs} = m_{tor} (\overline{OH} \times \boldsymbol{g}) + m_{pel} (\overline{PH} \times \boldsymbol{g}) \ . \tag{20}$$

Furthermore, to reduce the disturbance from the control of the torso, we compensate the driving torque (16) of the waist. Therefore, the total driving torque at hip in the PCS is,

$$\boldsymbol{\tau}_{lh\_pcs} = \boldsymbol{\tau}_{tr\_lh\_pcs} + \boldsymbol{\tau}_{gr\_lh\_pcs} + \boldsymbol{\tau}_{s\_w\_pcs} \ . \tag{21}$$

Let $\boldsymbol{z}_{y\_lh} \in R^{3\times1}$, $\boldsymbol{z}_{r\_lh} \in R^{3\times1}$, and $\boldsymbol{z}_{p\_lh} \in R^{3\times1}$ denote the direction vectors of yaw, roll, and pitch axes at the hip of the leading leg in the PCS respectively, the driving torques in the joint space of the hip can be calculated by,

$$\boldsymbol{\tau}_{lh} = \begin{bmatrix} \boldsymbol{z}_{y\_lh} & \boldsymbol{z}_{r\_lh} & \boldsymbol{z}_{p\_lh} \end{bmatrix}^{-1} \boldsymbol{\tau}_{lh\_pcs} \ . \tag{22}$$

VII. SIMULATION

A simulation has been conducted to verify the feasibility of the proposed method. The screen capture views, which are snapshotted in the stable walking phase, are shown in Fig. 6. The simulation system includes three reciprocally-connected modules, namely, the robot, the ground, and the controller. The robot model is of 27 DOFs, as shown in Fig. 1, and with the parameters listed in Table 1. First, the dynamics of the robot is constructed by the Newton Euler method, and a nonlinear spring-damper model is used to imitate the contact between the foot and the ground. These modules are updated in period of 10 microseconds. Second, the planning and servo control system is separated from the robot. The planning

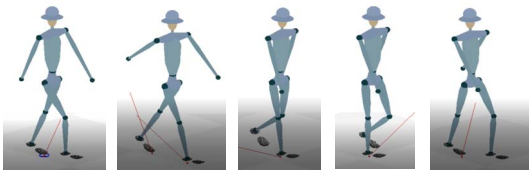

(a) 3D

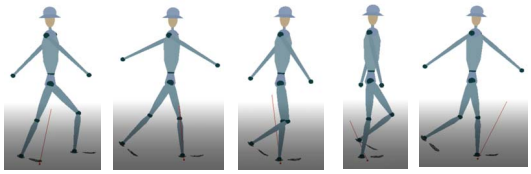

(b) In sagittal plane

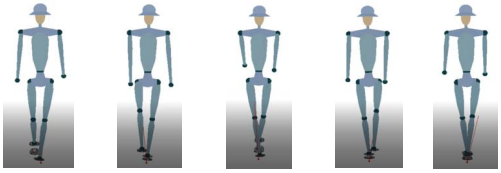

(c) In frontal plane

Fig. 6. Views of gait.

module gathers the sensor information and sends the control command with a period of 1 millisecond, and the control period of the servo system of the joints is 100 microseconds.

We conducted a 200-second walk simulation, which was divided into four phases: the first was the manual start phase. The robot accelerates from standstill to 0.69 m/s; the second is the acceleration phase, and the robot accelerates from 0.69 m/s to 0.83 m/s (3.0 km/h, equivalent to 3.64 km/h for a human being with 1.7m height) in 20 seconds with constant acceleration; and thereafter, the robot maintains the speed to the end.

The control parameters in the stable walking are regulated automatically: the control of ground-push uses the method proposed in this paper, and the general structure of the walking control and other control modules, such as the control swinging leg and the arms, are consistent with our previous work [9,10].

A. Walking stability

The robot achieves stable speed tracking during the constant speed walking, as shown in Fig. 7 (a). This prove that the proposed gait is stable. The desired speed is 0.83 m/s. There are small fluctuations in the actual speed, with a maximum of 0.89 m/s and a minimum of 0.78 m/s. The control error is within 7.2%. Figure 7 (b) shows the regulation of step length. Figure 7 (c) is the planned value of ground-push force, which is obtained by (3).

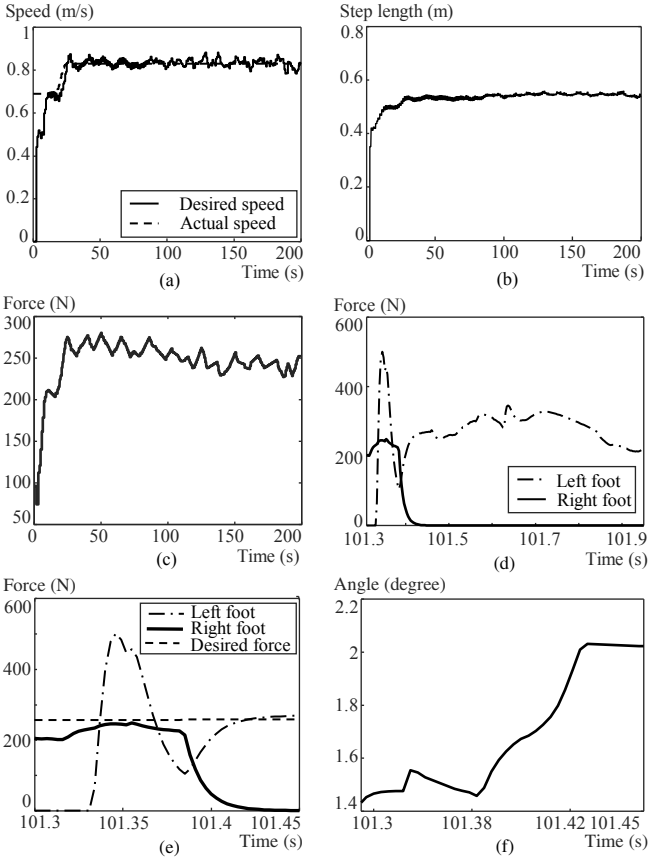

Fig. 7. Result of simulation. (a) Speed control. (b) Actual step length. (c) Desired push force. (d) Actual push force in 2 steps. (e) Value control of ground-push force. (f) Direction of ground-push force.

B. Performance of control of ground-push

A sample of stable walking is presented to show the performance of the ground-push, as shown in Fig. 7 (d). Among them, we enlarge the segment of DSP in Fig.7 (e), which presents the reaction force trajectories of the both legs after the landing of swing leg. In this period, the right leg is the rear leg. The result shows that the magnitude of the ground-push force is effectively controlled. Further, the direction of ground-push force, which is described by the angle between the force line and the line from COP of the trailing foot to the mass center of torso, is well controlled, as shown in Fig. 7 (f).

VIII. CONCLUSION AND DISCUSSION

The ground-push process, which is the main way of energy input of biped walking, is a complicated motion in which the torso, pelvis, front leg, and trailing leg are involved. First, this paper proposes a decentralized control method for dynamic walking, which is to divide the process into the module of ground-push, and the module of orientation control of robot. These modules are coordinated according to the phase of the robot motion. Second, a ground-push principle which is based on simplified model is presented. Further, the planning and control method is developed. A straight way walking simulation is conducted on a 27-DOF humanoid robot. The simulation shows that stable walking and speed tracking is achieved. The gait is very smooth and natural. However, there is room for improvement in speed tracking performance. Looking ahead, we will study learning methods to improve efficiency of biped walking.

REFERENCES

[1] McGeer T, "Passive dynamic walking," *Int. J. Robotics Res.* 9, 1990, pp. 62-82.

[2] Collins S H and Ruina A, "A bipedal walking robot with efficient and human-like gait," in *Proc. IEEE Conf. Robot. Automat.* (IEEE Press, Barcelona, Spain, 2005), pp. 1983-1988.

[3] Collins S, Ruina A, Tedrake R, Wisse M, "Efficient bipedal robots based on passive-dynamic walkers," *Science* 307 (5712), 2005, pp. 1082-1085.

[4] A. Goswami, B. Thuilot and B. Espiau, "A study of the passive gait of a compass-like biped robot: symmetry and chaos," *International Journal of Robotics Research*, 17 (12), 1998, pp. 1282-1301.

[5] Grizzle J W, Abba G and Plestan F, "Asymptotically stable walking for biped robots: analysis via systems with impulse effects," *IEEE Trans. Autom. Control* 46 (1), 2001, pp. 51-64.

[6] Westervelt E, Grizzle J, and Koditschek D, "Hybrid zero dynamics of planar biped walkers," *IEEE Trans. Autom. Control* 48 (1), 2003, pp. 42-56.

[7] Christine Chevallereau, J. W. Grizzle, "Asymptotically stable walking of a five-link underactuated 3-D bipedal robot," *IEEE Transaction on Robotics* 25(1), 2009, pp. 37-50.

[8] X. Luo, W. Li, C. Zhu, "Planning and control of COP-switch based planar biped walking," *J. Bionic Eng.* 8(1), 2011, pp. 33-48.

[9] Luo, Xiang, Zhu, Liqin, Xia, Lei, "Principle and method of speed control for dynamic walking biped robots," *Robotics and Autonomous Systems*, 66, 2015, pp. 129-144.

[10] Xiang Luo, Dan Xia, and Chi Zhu, "Impact dynamics-based torso control for dynamic walking biped robots," *International Journal of Humanoid Robotics*, Vol. 15, No. 3, 2018, 1850004.